ACS Combinatorial Science

Technology Note

pubs.acs.org/acscombsci

# High-Throughput Thermal Scanning for Protein Stability: Making a Good Technique More Robust

Shane A. Seabrook* and Janet Newman

Collaborative Crystallisation Centre (C3), Division of Materials Science and Engineering, Commonwealth Scientific and Industrial Research Organisation (CSIRO), Parkville, Victoria, Australia

Supporting Information

**ABSTRACT:** We present a high-throughput approach to help define experimental formulations that enhance protein stability, which is based on differential scanning fluorimetry (DSF). The method involves defining the thermal stability of a protein against a screen of 13 buffer systems, systematically sampling pH from 5.0 to 9.0 at high and low salt concentrations, using both redundancy and extensive controls to make the method robust. The screen allows rapid determination of a suitable base formulation for protein samples, and is particularly useful for difficult samples: those that are rapidly degraded or cannot be sufficiently concentrated for downstream analyses. Data obtained from three samples in this assay illustrate the vastly different values for thermal stability that can be obtained from different formulations. This approach is simple to interpret and reliable enough that it has been implemented as a service through the Collaborative Crystallisation Centre (C3).

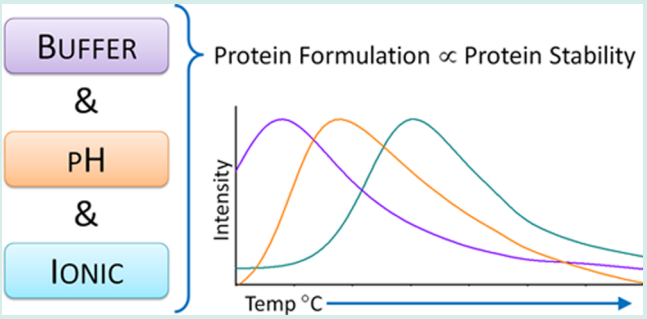


**KEYWORDS:** *differential scanning fluorimetry, protein stability, thermal shift assay, thermofluor, protein unfolding, formulation*

Completing many biophysical assays is often difficult because of the inherently unstable nature of proteins when they are purified and concentrated. Protein stability can often be enhanced by optimizing the formulation (formulation = a mixture of two or more chemicals) in which the protein sample is stored. Biochemists have historically utilized readily available tris- and phosphate-buffered saline formulas (TBS and PBS, respectively), with stepwise addition of ionic compounds, glycerol, reducing agents, polyols, and surfactants to increase the stability of a protein. This sequential method can work, but it is laborious and in many cases it does nothing but solvate a poorly folded protein.

Starting in the mid 1960s alternative buffer systems tuned to address the needs of biochemists (and their proteins) were developed by Good and co-workers.[1] Nowadays, a challenge is to find which of the numerous formulation options available is best for any given protein. Thermal stability as measured by differential scanning fluorimetry (DSF) is very well suited to this task. DSF fulfills four criteria for high-throughput screening: (1) low sample volume requirement, (2) high sample throughput, (3) ease of set up, and (4) rapid analysis. DSF monitors the response of an environmentally sensitive dye (SYPRO®) that is fluorescently active in a hydrophobic environment, for example, the core of an unfolded protein, and is quenched in an aqueous environment; the method is extensively described and compared in the literature.[3−7] The 'single point' measurement from this technique is correctly referred to as the temperature of hydrophobic exposure, $T_h$, which is defined as the minimum of the first derivative of a DSF melt curve. The value $T_h$ has been shown to have a high correlation to the absolute melt temperature, $T_m$, using orthogonal techniques such as differential scanning calorimetry.[8] By finding a formulation that increases the $T_h$ of a protein, we believe that we increase its conformational stability, which in turn should increase the long-term stability of the sample for biophysical assays, such as crystallisation, calorimetry, and spectroscopy. The Collaborative Crystallisation Centre (CSIRO C3) is a technology platform focusing on the production of protein crystals for diffraction experiments; as arguably the most important component of a crystallisation trial is the protein sample, being able to optimize the sample by adjusting the formulation is a powerful adjunct to the other technologies offered by C3.

**Development of the Buffer Screen and the Testing Protocol.** DSF gained popularity as a screening technique for ligand binding[4,5,9,10] and liquid formulation optimization for biologically active macromolecules.[3,8,11] Others have used it as a tool to quickly define and optimize the quality of protein preparations.[6,12−14] Our initial attempts at an in-house protein formulation screen shared many similarities with Ericsson et al.[15] and Niesen et al.,[4] and used a wide variety of buffers and small molecules. However, after nine iterations (thus the name

Received: January 28, 2013
Revised: April 30, 2013
Published: May 28, 2013




dx.doi.org/10.1021/co400013v | ACS Comb. Sci. 2013, 15, 387−392

"buffer screen 9"), we have narrowed the focus to a smaller set of components which we believe still provides enough variability to find specific formulations suitable for many soluble protein samples. As our goal with the DSF assay was for it to be a quick method of testing different formulations we use a rapid rate of heating (0.5 °C/30 s), and simply dilute the protein sample in the original buffer into the test solutions. The assay is performed in 96 well PCR plates where the total volume is 20 μL. Each (non control) sample contains protein, Sypro dye and a formulation: for protein samples of 1 mg/mL or more the relative volumes are 0.3 μL of protein, 0.3 μL of a 1:10 dilution of Sypro dye in water, and 19.4 μL of formulation. A more extensive description of the experiment is given in the Supporting Information. Although there is extensive literature showing that one can extract significant information from DSF experiments by altering parameters such as the rate of heating and the ratio of dye to protein, we have found that our standardized and basic approach provides enough information for our goal, and that the replication and inclusion of controls described as follows is the most powerful improvement to the assay.

There are two main rationales behind the design of the screen: *First*, limiting the formulation components to 15 buffers and sodium chloride minimizes incompatibility problems, yet still allows the buffer pH range from 5.0 to 9.0 to be sampled, with duplicate values at 6.0, 6.5, 7.0, and 7.5 (see Table 1 for a complete list of the formulations), at both low (50 mM) and high (200 mM) NaCl concentrations. The systematic arrangement of the formulations in the design lets us evaluate the dependence of the sample $T_h$ as a function of pH, salt concentration and the buffering chemical. *Second*, and more importantly, this paring down of components allows us to test conditions in triplicate and to include four controls, which greatly increases our confidence in the robustness of the method. The controls are (1) a benchmark control (the protein sample in its original formulation), (2 and 3) two negative controls (protein only control and dye only control), and (4) a positive control (a readily available protein with a known $T_h$). These controls allow us to rapidly determine a benchmark $T_h$, and estimate if the results from the assay are reliable or an artifact of the machine, some pathology of the sample, or interference from the DSF technique.

**Alternative Designs.** The formulation choices in our screen were selected to be compatible with the techniques used in structural biology, and are based on the chemicals readily available in a structural biology laboratory. The design can be modified for applications that call for different buffering chemicals and ionic agents; it is the controls, pH range, the testing of different buffering chemicals at the same pH, and perhaps most importantly, the systematic layout that are critical to the success of the screen design.

**Experiment Validation.** Figure 1a shows the responses from the four controls (described above) in a DSF experiment with endogluconase that was provided initially in TBS. The triplication of each measurement point ensures that the samples are reproducible: DSF is a low-information technique, which provides an estimation of the relative thermal stability of a protein sample, based on a nondirect measurement (i.e., we observe the fluorescence of dye, not the unfolding of a protein), thus it is important that the melt-curves are trustworthy. First, we ascertain that the positive control protein (in this case lysozyme, light blue curve) has behaved as expected. We find that 0.01 mg/mL lysozyme (Sigma L6876 dissolved in 50 mM tris chloride pH 8, 50 mM NaCl) gives a clear signal in the range of ~3000 ΔRFU and a $T_h$ value of 71 °C, consistent with previous experiments; if either of the values deviates significantly then it is an indication that there is something wrong with either the RT-PCR device or the dispensing robots, or some other part of the experiment, and that the experiment should be repeated after appropriate trouble shooting measures have been taken. The two negative controls (protein-only and

**Table 1. List of the Screen Contents and Their Corresponding Position[a]**

| position | contents | [NaCl] |
|---|---|---|
| A1, A2, A3 | lysozyme | n/a |
| A4, A5, A6 | water | 50 mM |
| A7, A8, A9 | water | 200 mM |
| A10, A11, A12 | protein control | n/a |
| B1, B2, B3 | sodium acetate | 50 mM |
| B4, B5, B6 | sodium acetate | 200 mM |
| B7, B8, B9 | piperazine | 50 mM |
| B10, B11, B12 | piperazine | 200 mM |
| C1, C2, C3 | MES (*N*-morpholino)ethanesulfonic acid) | 50 mM |
| C4, C5, C5 | MES (*N*-morpholino)ethanesulfonic acid) | 200 mM |
| C7, C8, C9 | sodium citrate | 50 mM |
| C10, C11, C12 | sodium citrate | 200 mM |
| D1, D2, D3 | bis tris | 50 mM |
| D4, D5, D6 | bis tris | 200 mM |
| D7, D8, D9 | ADA (*N*-(2-acetamido)iminodiacetic acid) | 50 mM |
| D10, D11, D12 | ADA (*N*-(2-acetamido)iminodiacetic acid) | 200 mM |
| E1, E2, E3 | imidazole | 50 mM |
| E4, E5, E6 | imidazole | 200 mM |
| E7, E8, E9 | MOPS (3-(*N*-morpholino)propanesulfonic acid) | 50 mM |
| E10, E11, E12 | MOPS (3-(*N*-morpholino)propanesulfonic acid) | 200 mM |
| F1, F2, F3 | HEPES (4-(2 hydroxyethyl) 1-piperazineethanesulfonic acid) | 50 mM |
| F4, F5, F6 | HEPES (4-(2 hydroxyethyl) 1-piperazineethanesulfonic acid) | 200 mM |
| F7, F8, F9 | $Na_2H/KH_2$ $PO_4$ | 50 mM |
| F10, F11, F12 | $Na_2H/KH_2$ $PO_4$ | 200 mM |
| G1, G2, G3 | tris chloride | 50 mM |
| G4, G5, G6 | tris chloride | 200 mM |
| G7, G8, G9 | glycyl-glycine | 50 mM |
| G10, G11, G12 | glycyl-glycine | 200 mM |
| H1, H2, H3 | sample benchmark | n/a |
| H4, H5, H6 | CHES (*N*-cyclohexyl-2-aminoethanesulfonic acid) | 50 mM |
| H7, H8, H9 | CHES (*N*-cyclohexyl-2-aminoethanesulfonic acid) | 200 mM |
| H10, H11, H12 | dye control | n/a |

[a]Available digitally on www.csiro.au/c3. These formulations here are geared toward protein crystallisation, however is would be easy to replace them with combinations appropriate for other techniques where the solvent requirements are different. The layout makes it easy to determine the effect that each formulation has on the protein sample.


dx.doi.org/10.1021/co400013v | *ACS Comb. Sci.* 2013, 15, 387−392

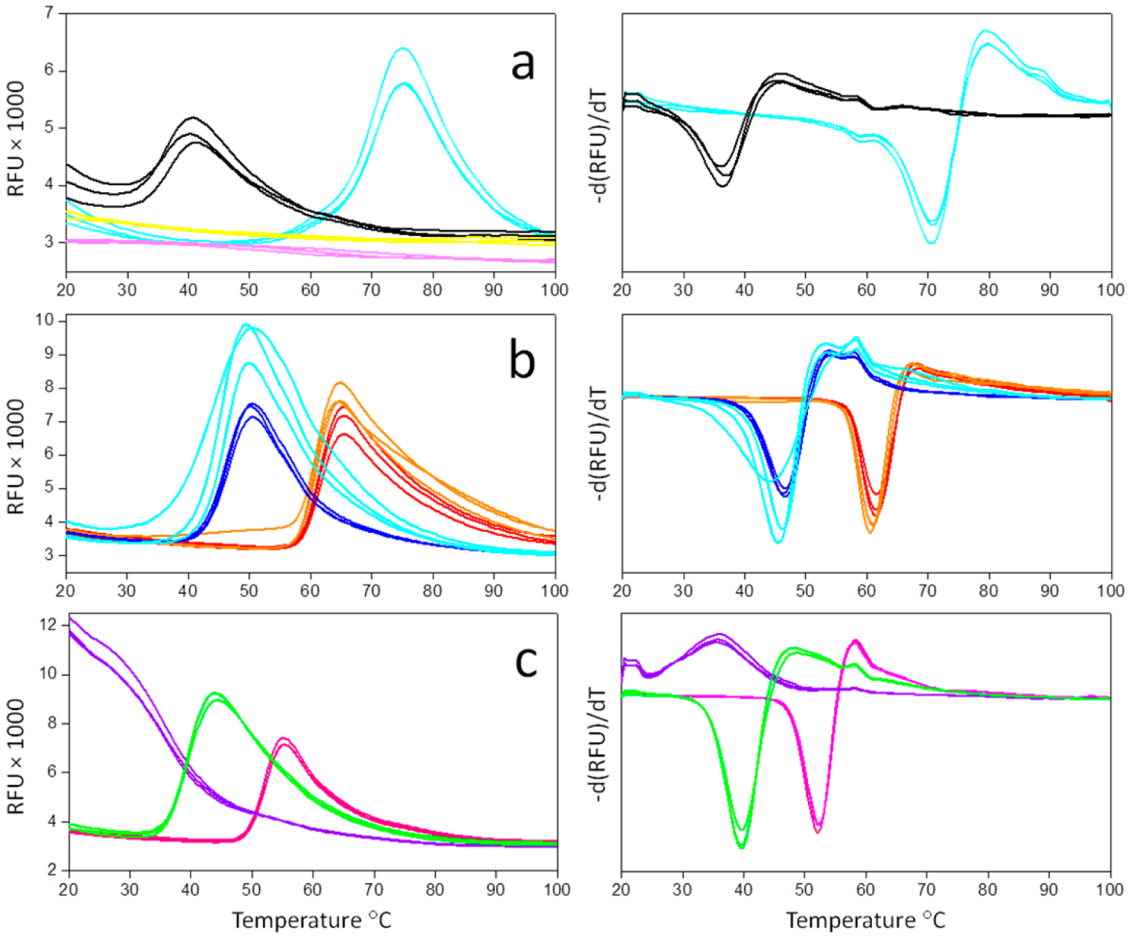


**Figure 1.** Selected melt curves from the thermofluor experiment for endogluconase (cellulase from *Aspergillus niger*, triplicate data are shown). The plots on the left-hand show the fluorescence response (RFU), with the first derivative of the melt curve shown on the right ($-d$(RFU)/dT). The negative peak of the first derivative is a good approximation of $T_h$. (a) Controls: lysozyme (light blue curve; $T_h$ 71.0 °C), protein only (pink curve; no event), dye only (yellow curve; no event), and endogluconase in TBS (black curve; $T_h$ 36.5 °C). (b) Buffered using 50 mM sodium acetate−acetic acid at pH 5.0 with 50 mM sodium chloride (red curve; $T_h$ 61.5 °C) and 200 mM (orange curve; $T_h$ 61.0 °C) NaCl. Unbuffered water with 50 mM (dark blue curve; $T_h$ 46.5 °C) and 200 mM (cyan curve; $T_h$ 45.0 °C) sodium chloride. (c) 50 mM bis-tris pH 6.5 (magenta curve; $T_h$ 52.0 °C), 50 mM HEPES pH 7.5 (green curve; $T_h$ 39.5 °C) and 50 mM CHES pH 9.0 (purple curve; $T_h$ not determined as there is no discernible peak on the derivative plot).

dye-only) (pink and yellow respectively) in the original protein formulation (here TBS) should return flat curves. These negative controls can serve as a valuable indicator for contaminated dye or PCR plates, naturally fluorescent samples or protein formulations. Finally, the black curve in Figure 1**a** is the control for endogluconase in TBS at pH 8.0, returning a benchmark $T_h$ of 36.5 ± 0.5 °C.

**Melt Curve Shapes.** Our interpretation of DSF is qualitative, with the goal of observing trends for the $T_h$ values rather than providing exact physical (kinetic or thermodynamic) values. The literature shows that attempts have been made to extract quantitative kinetic values and crystallizability scores from parametrizing DSF melt curves,[5,16] however these rely on having ideal or close to ideal melt curves, which happens all too infrequently in our experience. On the basis of the premise that the SYPRO dye fluoresces when exposed to the unfolded core of the protein, an ideal melt curve will exhibit a flat pretransition baseline, a steep transition on unfolding, and a slow decrease in signal after the maximum RFU is reached, much like the melt curves observed in Figure 1from, for example, bis-tris. Conversely, the melt curve resulting from a formulation based on CHES in Figure 1c is an excellent representation of an undesirable melt curve, with a high RFU response at 20 °C and no clear indication of an unfolding event; this curve suggests that the protein is largely mis-folded at 20 °C, and simply aggregates on heating, rather than unfolding. These two curves are two extremes, and there are many curve shapes in between.[12,13] Melt curve shape can be a more consistent predictor of downstream good behavior for a formulation than the $T_h$, and is particularly useful to consider in cases when different formulations result in similar melting temperatures.

We have found that in some cases the protein in the original formulation is in such a sorry state that the first round of buffer screening with DSF serves only to find an intermediate system in which the protein is folded well enough that the second, or subsequent, rounds of DSF (with the same buffer screen) can yield useful results.

**Finding a Better Formulation.** Given the assumption that there is a correlation between the temperature at which the protein unfolds and how stable it is in that formulation, the buffer screen 9 has been designed to test the effects of pH, type of buffer and ionic strength on the $T_h$ of a protein sample. The 3-fold replication used in buffer screen 9, while insufficient to


dx.doi.org/10.1021/co400013v | *ACS Comb. Sci.* 2013, 15, 387−392

**a)**

| | 1 | 2 | 3 | 4 | 5 | 6 | 7 | 8 | 9 | 10 | 11 | 12 |
|---|---|---|---|---|---|---|---|---|---|---|---|---|
| A | Lysozyme | Lysozyme | Lysozyme | 46.50 | 46.50 | 46.50 | 45.50 | 44.00 | 46.00 | Protein CTRL | Protein CTRL | Protein CTRL |
| B | 61.50 | 61.50 | 61.50 | 60.50 | 61.00 | 61.00 | 60.00 | 60.00 | 60.00 | 59.50 | 60.00 | 60.00 |
| C | 56.00 | 57.50 | 58.00 | 56.50 | 55.00 | 56.50 | 54.00 | 54.00 | 53.50 | 55.00 | 54.50 | 55.00 |
| D | 54.00 | 54.00 | 53.50 | 52.00 | 52.00 | 52.50 | 50.00 | 50.50 | 50.00 | 50.50 | 50.50 | 51.00 |
| E | 46.50 | 47.00 | 46.50 | 45.50 | 45.50 | 45.50 | 46.00 | 47.00 | 47.00 | 46.50 | 46.50 | 46.50 |
| F | 40.50 | 41.00 | 44.00 | 39.50 | 39.50 | 39.50 | 42.00 | 40.50 | 39.50 | 40.50 | 40.00 | 40.50 |
| G | 35.00 | 36.00 | 35.00 | 36.00 | 32.50 | 38.00 | 26.00 | 25.50 | 25.00 | *null value* | *null value* | *null value* |
| H | 37.00 | 36.00 | 36.50 | *null value* | *null value* | *null value* | *null value* | *null value* | *null value* | Dye CTRL | Dye CTRL | Dye CTRL |

**b)**

| | 1 | 2 | 3 | 4 | 5 | 6 | 7 | 8 | 9 | 10 | 11 | 12 |
|---|---|---|---|---|---|---|---|---|---|---|---|---|
| A | Lysozyme | Lysozyme | Lysozyme | 64.00 | 63.00 | 64.00 | 64.00 | 64.00 | 64.00 | Protein CTRL | Protein CTRL | Protein CTRL |
| B | 48.00 | 48.00 | 48.00 | 47.50 | 47.00 | 47.50 | 59.00 | 59.00 | 59.00 | 59.50 | 59.50 | 60.00 |
| C | 62.50 | 62.50 | 62.50 | 62.50 | 62.50 | 62.50 | 64.50 | 65.00 | 65.00 | 65.00 | 65.00 | 65.00 |
| D | 64.50 | 64.50 | 64.50 | 64.50 | 64.50 | 64.50 | 65.50 | 65.50 | 65.50 | 65.00 | 65.00 | 65.50 |
| E | 64.50 | 64.50 | 64.50 | 64.50 | 64.50 | 64.00 | 63.50 | 65.00 | 64.50 | 64.50 | 65.00 | 65.00 |
| F | 65.00 | 64.00 | 65.00 | 64.50 | 64.50 | 64.50 | 65.00 | 65.00 | 64.50 | 64.50 | 64.50 | 64.50 |
| G | 64.50 | 64.50 | 64.50 | 64.50 | 64.00 | 64.00 | 64.50 | 64.50 | 64.50 | 64.50 | 64.00 | 64.50 |
| H | 65.00 | 65.00 | 65.00 | 63.00 | 63.00 | 63.00 | 63.00 | 63.00 | 63.00 | Dye CTRL | Dye CTRL | Dye CTRL |

**c)**

| | 1 | 2 | 3 | 4 | 5 | 6 | 7 | 8 | 9 | 10 | 11 | 12 |
|---|---|---|---|---|---|---|---|---|---|---|---|---|
| A | Lysozyme | Lysozyme | Lysozyme | 46.5 | 47.5 | 47.0 | 48.0 | 47.0 | 48.5 | Protein CTRL | Protein CTRL | Protein CTRL |
| B | 36.0 | 36.5 | 36.5 | 36.0 | 36.0 | 35.0 | 41.0 | 40.5 | 40.5 | 42.0 | 42.0 | 42.0 |
| C | 44.5 | 44.0 | 43.0 | 44.5 | 46.0 | 44.0 | 44.5 | 45.0 | 45.5 | 46.0 | 46.5 | 46.5 |
| D | 46.5 | 46.5 | 44.0 | 48.5 | 48.5 | 48.5 | 48.5 | 48.0 | 48.5 | 49.5 | 49.5 | 50.0 |
| E | 48.0 | 48.0 | 47.0 | 50.0 | 50.0 | 48.0 | 48.5 | 49.0 | 49.0 | 51.0 | 50.5 | 50.5 |
| F | 51.0 | 50.5 | 50.5 | 53.0 | 53.0 | 52.5 | 51.5 | 51.5 | 50.5 | 53.5 | 53.5 | 53.0 |
| G | 51.5 | 52.0 | 51.5 | 53.0 | 52.5 | 52.5 | 50.5 | 51.0 | 50.5 | 53.0 | 52.0 | 54.0 |
| H | 50.5 | 50.5 | 50.0 | 49.5 | 49.5 | 49.5 | 51.5 | 52.0 | 52.0 | Dye CTRL | Dye CTRL | Dye CTRL |

**Figure 2.** These three heat maps indicate the vastly different response that three example samples can have to the formulations in buffer screen 9: (a) endogluconase, (b) transferase, and (c) amidase. The median color (yellow) corresponds to the benchmark $T_h$, red the highest $T_h$ value, and blue the lowest $T_h$.

enable a statistically rigorous analysis, does lead to an increase in confidence in the results obtained. Our experience suggests that the inherent noise in our experimental system is on the order of ±1 °C, so that $T_h$ changes of >1 °C become interesting. Figure 1b and 1c shows representative subset of the melt curves, and corresponding derivatives, from a DSF experiment on endogluconase. Observation of the curves in Figure 1b resulting from formulations of 50 mM NaCl (red curve) and 200 mM NaCl (orange curve) with 50 mM sodium acetate-acetic acid at pH 5.0 show a $T_h$ value of 61.5 °C which is a 25 °C increase from the benchmark $T_h$, one of the largest temperature shifts we have observed. Combining this large shift in $T_h$ with the nearly ideal shape of the denaturation curve engendered by acetate, we draw the conclusion that endogluconase is more stable at the low pH, in particular in acetate buffers at low pH, than in neutral or high pH.

**Response for Different Proteins.** Figure 2 shows heat maps for endogluconase, an amidase (allophanate hydrolase (AtzF) from *Pseudomonas* SP) and a transferase (acetylglucosaminyltransferase (AstC) from *Escherichia coli*). The heat maps are one-dimensional, comparing only the $T_h$ between formulations. However, the heat maps provide an efficient way to compare the $T_h$ response for various proteins across all formulations in buffer screen 9 (Table 1 shows the condition in each cell of the heat map); AtzF and AstC were selected as examples as all formulations return a clearly defined $T_h$ value for these two proteins. Looking at the three maps in Figure 2 it is immediately obvious how differently the three samples respond to the changes in formulation.

The $T_h$ for endogluconase (Figure 2a) shows a remarkable dependence on the pH with very little difference between the chemicals that create that pH, and a marginal preference for the lower concentration of NaCl. Unlike many proteins, endogluconase has a strong preference for formulations with a low pH, being most stable in sodium acetate at pH 5.0. In our experience, sodium acetate often returns melt curves with no discernible features or with comparatively low $T_h$ values. The transferase (Figure 2b) has a far more limited $T_h$ response across buffer screen 9, with no obvious "best" formulation (ADA at pH 6.5 with 50 mM NaCl is 0.5 °C more stable than the sample benchmark, and thus is within the expected noise of the experiment). What is interesting is that the $T_h$ value is almost constant from pH 6.0 to pH 8.5, with no discernible preference between high and low salt concentrations. This transferase demonstrates the commonly observed response to acetate buffers. This response seems to be a result of the acetate


dx.doi.org/10.1021/co400013v | *ACS Comb. Sci.* 2013, 15, 387−392

buffer rather than the pH, as a shift to piperazine at pH 5.5 (only half a pH unit) increases the $T_h$ by over 10 °C. The amidase (Figure 2c) appears to be most stable between pH 7.5 and 8.5, with a clear preference for 200 mM NaCl across almost all formulations. Much like the transferase, the amidase appears to be easily destabilized at low pH, in particular when buffered with acetate. Unlike the amidase, the increase in $T_h$ is graduated evenly until a pH of 7.5 is reached.

**Dynamic Light Scattering.** To confirm the results of the DSF experiment, we recommend assessing a select few formulations (the best, the worst, the benchmark control) using a technique that provides orthogonal data; we use dynamic light scattering (DLS), which can rapidly assess the aggregation propensity of a biomacromolecule.[17,18] The distributions in Figure 3 result from endogluconase in three

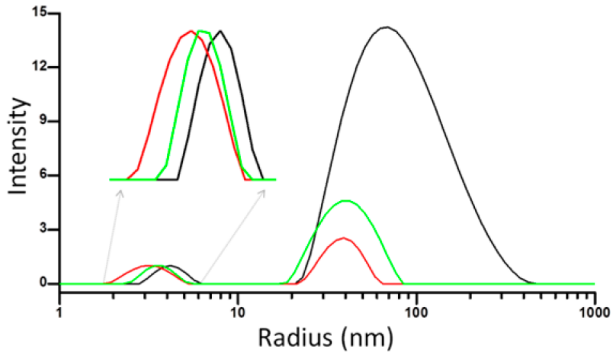


**Figure 3.** Select DLS distributions to illustrate an orthogonal view of the protein stability in various formulations. Insert shows magnification of the low molecular weight species, normalized for intensity value. TBS (green distribution): Peak 1 radius = 3.7 nm; % mass = 98.8; % Pd = 12. Peak 2 radius = 43 nm; % mass =1.2; % Pd = 28. Acetate at pH 5.0 (red distribution): Peak 1 radius = 3.4 nm; % mass = 99.8; % Pd = 18. Peak 2 Radius = 47 nm; % Mass = 0.2; % Pd = 26. CHES at pH 9.0 (black distribution): Peak 1 Radius = 4.8 nm; % mass = 63; % Pd =17. Peak 2 radius = 84 nm; % mass = 37; % Pd = 48.

different buffer conditions, namely the control formulation (Figure 3; green curve, TBS), the best formulation (Figure 3; red curve, acetate at pH 5.0) and the worst formulation (Figure 3; black curve, CHES at pH 9.0). The DLS signal intensity is inversely proportional to the hydrodynamic volume (size) of the molecule, and as such it appears that all three formulations create a large aggregate.[19] However, normalizing the peak associated with the active species, and observing the calculated percent mass (determined by the DLS software, see Supporting Information), we can quantify how much of the sample is responsible for the signal. The percent mass in both the control and the acetate formulations is ~99% low hydrodynamic radius species, which is in alignment with the MW for a monomer of endogluconase (~75 kDa). Combining this with the knowledge that the protein returns a significantly increased $T_h$ in acetate at pH 5.0 over the TBS provides assurance that we are suggesting the most appropriate formulation. Looking at the distribution that arises from endogluconase in CHES, it is immediately obvious that there is a significant increase in the quantity of aggregate, and the low size species is not the same size as those in TBS or acetate; when we combine this with the information provided from the DSF experiment, we can strongly suggest that the DLS experiment is showing us the presence of a partially unfolded monomer and a non specific aggregate, verifying that CHES at pH 9.0 would not be a suitable formulation in this instance.

**Summary.** We have found that a systematic design and the introduction of rigorous controls and replication into an otherwise routine melting protocol using the technique of DSF for protein stability has proven to be very useful, and allows the results from a single experiment to be adopted with confidence. The formulations in buffer screen 9 allows rapid determination of a desirable base formulation for any given protein directly from the purification and concentration stage, which provides an excellent point from which to refine protein stability by fine screening around that formulation and using appropriate additives, or for immediate application to one of the numerous biophysical assays available. This design has been used for assaying over 50 samples in the last year, with subtle adaptations being applied to many more, and is now included in the range of technologies available to the C3 (www.csiro.au/c3) user community.

## ■ ASSOCIATED CONTENT

### Ⓢ Supporting Information

Comprehensive description of the method for preparing the combinatorial formulation screen and setting up the DSF and DLS experiments. This material is available free of charge via the Internet at http://pubs.acs.org.

## ■ AUTHOR INFORMATION

### Corresponding Author

*Postal Address: CSIRO Collaborative Crystallisation Centre (C3), 343 Royal Parade, Parkville, Victoria, Australia 3052. Telephone: +61 396627361. Website: http://www.csiro.au/c3. E-mail: shane.seabrook@csiro.au.

### Notes

The authors declare no competing financial interest.

## ■ ACKNOWLEDGMENTS

We thank Drs. Brendon Monahan and Jessica Welch for providing numerous samples of *N. aspergillis* endogluconase, and the many colleagues who provided a steady stream of proteins for melt analysis that have allowed us to refine the methodology. We are grateful to Dr. Thomas Peat for critical reading of the manuscript and Dr. Olan Dolezal and Mr. Dane Vassiliadis for manuscript review. The collaborative crystallisation centre (C3) is an ISO 17025 certified (accredited by the National Association of Testing Authorities, Australia) core technology platform fully funded by the Materials Science and Engineering division of the Commonwealth Scientific and Industrial Research Organisation (CSIRO).

## ■ REFERENCES

(1) Good, N. E.; Winget, G. D.; Winter, W.; Connolly, T. N.; Izawa, S.; Singh, R. M. M. Hydrogen Ion Buffers for Biological Research. *Biochemistry* **1966**, *5* (2), 467−477.

(2) Steinberg, T. H.; Jones, L. J.; Haugland, R. P.; Singer, V. L. SYPRO Orange and SYPRO Red Protein Gel Stains: One-Step Fluorescent Staining of Denaturing Gels for Detection of Nanogram Levels of Protein. *Anal. Biochem.* **1996**, *239* (2), 223−237.

(3) Goldberg, D. S.; Bishop, S. M.; Shah, A. U.; Sathish, H. A. Formulation Development of Therapeutic Monoclonal Antibodies Using High-Throughput Fluorescence and Static Light Scattering Techniques: Role of Conformational and Colloidal Stability. *J. Pharm. Sci.* **2011**, *100* (4), 1306−1315.

(4) Niesen, F. H.; Berglund, H.; Vedadi, M. the Use of Differential Scanning Fluorimetry to Detect Ligand Interactions That Promote Protein Stability. *Nat. Protoc.* **2007**, *2* (9), 2212−2221.
(5) Pantoliano, M. W.; Petrella, E. C.; Kwasnoski, J. D.; Lobanov, V. S.; Myslik, J.; Graf, E.; Carver, T.; Asel, E.; Springer, B. A.; Lane, P.; Salemme, F. R. High-Density Miniaturized Thermal Shift Assays as a General Strategy for Drug Discovery. *J. Biomol. Screen.* **2001**, *6* (6), 429−440.
(6) Phillips, K.; de la Pena, A. H. The Combined Use of the Thermofluor Assay and Thermoq Analytical Software for the Determination of Protein Stability and Buffer Optimization As an Aid in Protein Crystallization. *Curr. Protoc. Mol. Biol.* **2011**, *10*, 10-28.
(7) Vedadi, M.; Arrowsmith, C. H.; Allali-Hassani, A.; Senisterra, G.; Wasney, G. A. Biophysical Characterization of Recombinant Proteins: A Key to Higher Structural Genomics Success. *J. Struct. Biol.* **2010**, *172* (1), 107−119.
(8) He, F.; Hogan, S.; Latypov, R. F.; Narhi, L. O.; Razinkov, V. I. High Throughput Thermostability Screening of Monoclonal Antibody Formulations. *J. Pharm. Sci.* **2010**, *99* (4), 1707−1720.
(9) Senisterra, G. A.; Finerty, P. J. High Throughput Methods of Assessing Protein Stability and Aggregation. *Mol. BioSyst.* **2009**, *5* (3), 217−223.
(10) Vedadi, M.; Niesen, F. H.; Allali-Hassani, A.; Fedorov, O. Y.; Finerty, P. J., Jr.; Wasney, G. A.; Yeung, R.; Arrowsmith, C.; Ball, L. J.; Berglund, H.; Hui, R.; Marsden, B. D.; Nordlund, P.; Sundstrom, M.; Weigelt, J.; Edwards, A. M. Chemical Screening Methods to Identify Ligands That Promote Protein Stability, Protein Crystallization, And Structure Determination. *Proc. Natl. Acad. Sci.* **2006**, *103* (43), 15835−40.
(11) He, F.; Woods, C. E.; Trilisky, E.; Bower, K. M.; Litowski, J. R.; Kerwin, B. A.; Becker, G. W.; Narhi, L. O.; Razinkov, V. I. Screening of Monoclonal Antibody Formulations Based on High-Throughput Thermostability and Viscosity Measurements: Design of Experiment and Statistical Analysis. *J. Pharm. Sci.* **2011**, *100* (4), 1330−1340.
(12) Crowther, G. J.; He, P.; Rodenbough, P. P.; Thomas, A. P.; Kovzun, K. V.; Leibly, D. J.; Bhandari, J.; Castaneda, L. J.; Hol, W. G. J.; Gelb, M. H.; Napuli, A. J.; Van Voorhis, W. C. Use of Thermal Melt Curves to Assess the Quality of Enzyme Preparations. *Anal. Biochem.* **2010**, *399* (2), 268−275.
(13) Crowther, G. J.; Napuli, A. J.; Thomas, A. P.; Chung, D. J.; Kovzun, K. V.; Leibly, D. J.; Castaneda, L. J.; Bhandari, J.; Damman, C. J.; Hui, R.; Hol, W. G. J.; Buckner, F. S.; Verlinde, C.; Zhang, Z. S.; Fan, E. K.; Van Voorhis, W. C. Buffer Optimization of Thermal Melt Assays of Plasmodium Proteins for Detection of Small-Molecule Ligands. *J. Biomol. Screen.* **2009**, *14* (6), 700−707.
(14) Uniewicz, K. A.; Ori, A.; Xu, R. Y.; Ahmed, Y.; Wilkinson, M. C.; Fernig, D. G.; Yates, E. A. Differential Scanning Fluorimetry Measurement of Protein Stability Changes upon Binding to Glycosaminoglycans: A Screening Test for Binding Specificity. *Anal. Chem.* **2010**, *82* (9), 3796−3802.
(15) Ericsson, U. B.; Hallberg, B. M.; DeTitta, G. T.; Dekker, N.; Nordlund, P. Thermofluor-Based High-Throughput Stability Optimization of Proteins for Structural Studies. *Anal. Biochem.* **2006**, *357* (2), 289−298.
(16) Zucker, F. H.; Stewart, C.; Rosa, J. d.; Kim, J.; Zhang, L.; Xiao, L.; Ross, J.; Napuli, A. J.; Mueller, N.; Castaneda, L. J.; Nakazawa Hewitt, S. R.; Arakaki, T. L.; Larson, E. T.; Subramanian, E.; Verlinde, C. L. M. J.; Fan, E.; Buckner, F. S.; Van Voorhis, W. C.; Merritt, E. A.; Hol, W. G. J. Prediction of Protein Crystallization Outcome Using a Hybrid Method. *J. Struct. Biol.* **2010**, *171* (1), 64−73.
(17) Braginskaya, T. G.; Dobitchin, P. D.; Ivanova, M. A.; Klyubin, V. V.; Lomakin, A. V.; Noskin, V. A.; Shmelev, G. E.; Tolpina, S. P. Analysis of the Polydispersity by Photon Correlation Spectroscopy. Regularization Procedure. *Phys. Scr.* **1983**, *28* (1), 73.
(18) Kadima, W.; McPherson, A.; Dunn, M. F.; Jurnak, F. A. Characterization of Precrystallization Aggregation of Canavalin by Dynamic Light Scattering. *Biophys. J.* **1990**, *57* (1), 125−132.
(19) Gulari, E.; Gulari, E.; Tsunashima, Y.; Chu, B. Photon Correlation Spectroscopy of Particle Distributions. *J. Chem. Phys.* **1979**, *70* (8), 3965−3972.